



The effect of polypropylene fiber on the curing time of class G oil well cement and its mechanical, petrophysical, and elastic properties

Abdulmalek Ahmed¹ · Ahmed Abdulhamid Mahmoud¹ · Salaheldin Elkatatny¹

Received: 14 February 2022 / Accepted: 30 December 2022 / Published online: 16 January 2023
© The Author(s) 2023

Abstract

The cement paste is subjected to various loads throughout a well's life, which may compromise some of its essential characteristics and impair its performance. When the cement paste is first being formed and the cement's characteristics have not yet fully matured, these loadings take on greater importance. In this study, the early properties of cement used in oil wells that contains polypropylene fiber are assessed. Five different curing times were used to prepare ten cement samples (6, 12, 24, 48, and 72 h). Five samples contained polypropylene fiber, while the remaining five samples were without polypropylene fibers. After the samples were prepared, the examination of several early cement properties took place. Nuclear magnetic resonance (NMR) was used to describe each sample in order to determine how the curing times affected the cement's porosity. The findings demonstrated that both cement systems' compressive and tensile strengths increased with curing time, and that adding polypropylene fiber enhanced the cement's strength. The porosity and permeability of the cement specimens were significantly reduced with the incorporation of polypropylene fibers, as well as with time during the curing process for both cement samples. The reduction of Young's modulus and the increase in Poisson's ratio show that the addition of polypropylene fibers also makes the cement more elastic. To express variations in porosity as well as compressive and tensile strengths, logarithmic relationships were constructed. While the Poisson's ratio, Young's modulus, density variations, and permeability were precisely modeled by power-law equations.

Keywords Oil well cement · Cement properties · Curing time · Polypropylene fiber

List of symbols

DV	Density variation (%)
E_s	Static Young's modulus (GPa)
K	Permeability (mD)
ϕ	Porosity (%)
T	Curing time (hours) (MPa)
TS	Tensile strength (MPa)
UCS	Unconfined compressive strength
ν	Poisson ratio

Acronyms

°F	Degree Fahrenheit
μm	Micrometre
API	American petroleum institute
ASTM	American society for testing and materials
BWOC	By weight of cement
CDF	Cumulative distribution function
mD	Millidarcy
MHz	Megahertz
MPa	Megapascal
NMR	Nuclear magnetic resonance
PDF	Pore distribution function
PPF	Polypropylene fiber cement
R^2	Correlation coefficients
T_2	Relaxation time
XRF	X-ray fluorescence

✉ Salaheldin Elkatatny
elkatatny@kfupm.edu.sa

Abdulmalek Ahmed
g201080240@kfupm.edu.sa

Ahmed Abdulhamid Mahmoud
ahmed.mahmoud@kfupm.edu.sa

¹ College of Petroleum Engineering and Geosciences, King Fahd University of Petroleum & Minerals, Dhahran 31261, Saudi Arabia

Introduction

In the oil and gas industry, when the steel casing is used to tolerate the collapse and burst forces, a cement slurry is utilized to fill the annulus (Nelson and Guillot 2006). The formation of the cement sheath occurs as the slurry progressively begins to harden. The cement sheath is crucial to the well's integrity because it prevents fluid from moving between distinct formations, provides zonal isolation, shields the casing string from corrosion, and supports the casing and the drilled zones mechanically. In the worst-case scenarios, the breakdown of the cement paste could result in annulus pressurization, formation fluid migration to the surface, and blowout. Formulating a high-performance cement paste that guarantees the well's fundamental integrity, lowers the hazard of failure from accumulated materials formed by the physicochemical process, could help to lessen the risk of cement failure (Krakowiak et al. 2015).

Recently, several researchers evaluated the addition of several kinds of fibers such as silicic, organic, wollastonite, and monofilament fibers to the cement slurry to raise the well's useful life duration, enhance cement performance, and reduce costs associated with the cement matrix failures by improving the strength and minimizing the circulation loss of the cement (Shi et al. 1995; Elmoneim et al. 2000; Ilyas et al. 2012; Al Maskary et al. 2014; Iremonger et al. 2015).

One of these fibers is polypropylene which is a synthetic fiber that had been used by many researchers to enhance the failure parameters (compressive and tensile strength) of the soil (Yetimoglu et al. 2005; Tang et al. 2007; Viswanadham et al. 2009) and minimizing its shrinkage (Puppala and Musenda 2000; Vasudev 2007). Moreover, polypropylene fiber had been added to overcome the issue of cement brittleness in the concrete industry. In which cementitious materials are known to be brittle with less strain capacity and tensile strength (Yao et al. 2003; Vandewalle 2007; Jamshidi and Karimi 2019; Bentur and Mindess 2020). The major mechanism of the polypropylene fiber is by forming a mesh network that could mitigate circulation loss of the cement as well as reduce the permeability of the cement. Polypropylene fiber could also increase the strength and durability of the cement. In addition, the shrinkage cracking and the propagation of the micro-cracks could be minimized (Messier et al. 2002). For the oil and gas industry, several studies were published currently regarding the application of polypropylene fiber in well cementing to enhance the properties of Class G cement (Ahmed et al. 2018; Elkatatny et al.

2020) and improve its carbonation resistance (Mahmoud and Elkatatny 2020).

The hydration process causes the cement paste, which is a porous substance, to gradually transition from a liquid to a solid form. Depending on the well depth, different slurries with different compositions may be used during the cementing process, and their hydration occurs under varying temperatures, pressure, and time circumstances. Following the creation of the cement slurry, the qualities of the cement paste depend on many factors (Agofack et al. 2019).

Additionally, the cement paste is subjected to various mechanical and thermal loads during an oil well's life, which may compromise the cement sheath's structural integrity. While the pressure varies throughout the casing test from 10 to 80 MPa depending on the kind of reservoir, it could reach more than 40 MPa when drilling oil wells (Thiercelin et al. 1997). These loads may cause cracks to occur at the casing cement or rock cement interface as a result of the cement sheath deforming. This is particularly important when these loads are implemented early in the curing process before the cement's mechanical characteristics and strength have fully developed. Whereas the majority of causes of well leaks are known to be cement shrinkage and early reduction in pore pressure (Parcevaux and Sault 1984; Lyomov et al. 1997). Nevertheless, only a small number of experimental researches were conducted to assess the hydration of the wellbore cementing under harsh conditions and at various curing durations. The majority of these studies focused solely on elastic parameters like Poisson's ratio and Young's modulus or mechanical properties like compressive and tensile strengths (Reinås et al. 2011; Mahmoud and Elkatatny 2019). However, the effects on porosity and permeability, as well as the variation in cement properties with the growth of the early curing times, were not evaluated in the previous studies. These properties are crucial, particularly for new cement formulations like the cement containing polypropylene fibers that are taken into account in this study.

The early age characteristics of the cement paste can be investigated using a variety of experimental techniques. Some of these techniques concentrate on the reaction rate, while others examine the cement's chemical or physical characteristics over time (Parrott et al. 1990; Sant et al. 2009). This study compares cement made with and without polypropylene fiber to see how the properties of the cement matrix changed early in the hydration process. During the first 3 days of curing, a series of tests were assessed. Nuclear magnetic resonance (NMR) was used to analyze all cement samples in order to better understand how cement porosity changed over the time of curing.

Experimental program

Materials

Class G cement, polypropylene fiber, and other chemical additions that increase cement's characteristics and make it useable in a variety of wellbore circumstances make up the bulk of the study's components. These additives include silica flour, deformers, dispersants, and fluid loss agents. The co-authors, who provided extensive information on the mechanical, petrophysical, elastic, thermal,

and microstructure properties, used this Class G cement (Mahmoud et al. 2018; Ahmed et al. 2021b, c; Bageri et al. 2021).

The wet dispersion unit ANALYSETTE 22 Nano Tec plus instrument was used to determine the particle size distribution for the Class G cement powder. According to the findings, the cement's median particle size is 20.9 μm, and 90% of cement particles are smaller than 47 μm, as presented in Fig. 1.

The X-ray fluorescence (XRF)-derived elemental compositions show that class G cement has a high amount of calcium and a moderate quantity of silicon of around 72% and 12%, respectively, as depicted in Fig. 2.

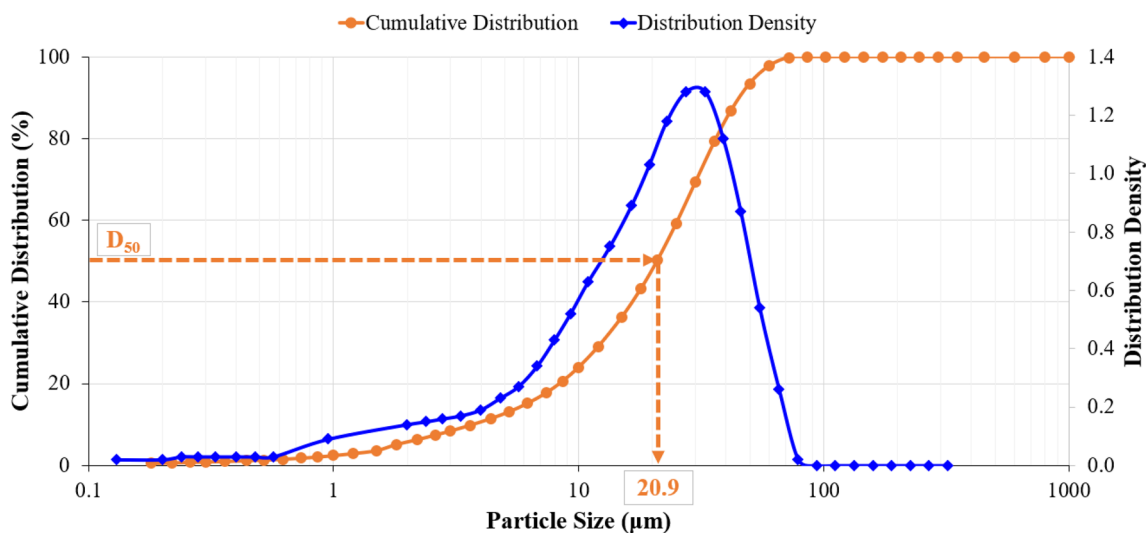


Fig. 1 Class G cement's distribution of particle sizes

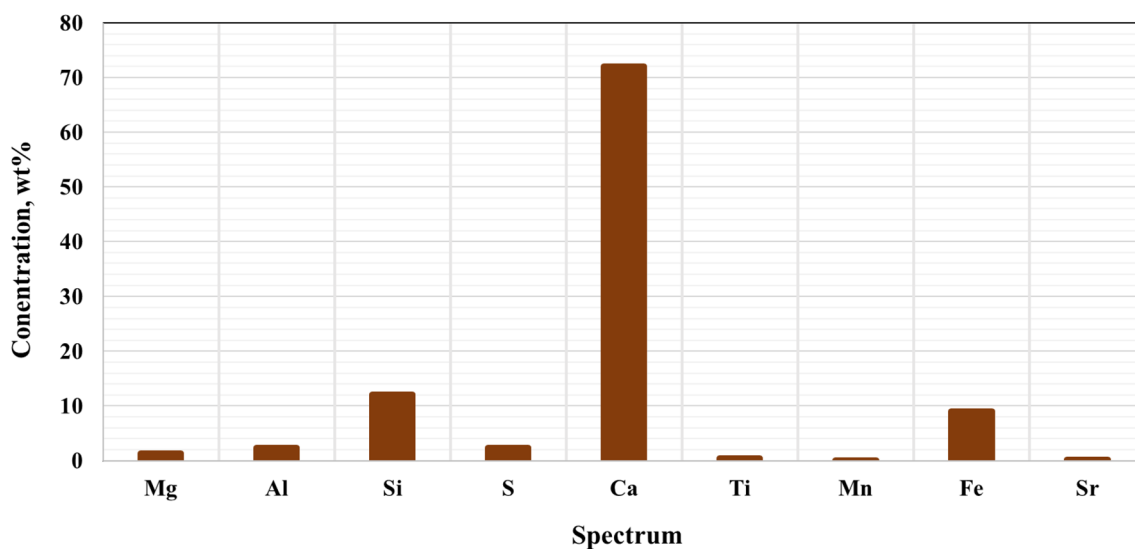


Fig. 2 Class G cement's composition performed by XRF



Fig. 3 Shape of the polypropylene fibers

The polypropylene fiber utilized in this study is a synthetically modified polypropylene fiber which has a triangular shape as presented in Fig. 3, this shape makes the polypropylene fiber to have a larger surface area (Park et al. 2003; Liu et al. 2012). Due to the larger surface area, polypropylene fiber can speed up the cement's hydration kinetics (Sobolev and Gutiérrez 2005; Thomas et al. 2009). By quickly filling the gap between the cement grains with hydrated phases, this process induces matrix densification and accelerates the improvement of compressive strength while reducing cement matrix porosity (Jo et al. 2007).

Slurries preparation

The API standards (API 1997) were used to prepare the cement slurries. The neat cement was made up of Class G cement, 2.82 10^{-6} % by weight of cement (BWOC) of defoamer, 44% BWOC water, 0.7% BWOC fluid loss, 35% BWOC silica flour, 0.1% BWOC expandable material, and 0.08% BWOC dispersant. The polypropylene-based cement slurry was created by adding 0.125% BWOC of polypropylene fiber in addition to the additives taken into consideration to create the neat slurry. This concentration of polypropylene fiber was taken into consideration in accordance with the recommendation of Elkhatny et al. (2020). It should be mentioned that silica flour is usually used at a temperature of more than 230 °F. However, in this work, we used silica flour to make sure that both cement systems for the base and polypropylene cement samples have high compressive strength and tensile strength.

Experimental techniques

Following preparation, all of the slurries were put into cylindrical and cubical molds in accordance with the required tests. The samples were then allowed to cure for varying amounts of time—6, 12, 24, 48, and 72 h—in water baths filled with distilled water heated to 170 °F. Following each curing period, samples of the neat cement and the polypropylene-based cement were taken out of the molds and put through a number of tests.

Failure tests

To explore the effect of hydration on the strength of the polypropylene specimens, compressive and tensile strengths were assessed for all specimens following the various curing periods. According to the ASTM standard (ASTM 2020), cube-shaped cement samples with 2.0-inch edges were utilized for the compressive strength test. With a cylindrical specimen that was 1.5 inches in diameter and 0.75 inches thick, the Brazilian test for tensile strength was carried out in accordance with (ASTM 2001) standard. Every cement sample's compressive and tensile strength was measured on three different specimens at a given curing period, and the average of those three readings was used to determine the cement sample's compressive or tensile strength.

Petrophysical tests

To determine how the curing time affected the petrophysical characteristics of the polypropylene specimens, the porosity and permeability of all the specimens taken into consideration in this work were assessed at the various curing periods. For the evaluation of petrophysical parameters, samples with dimensions of 1.5 inches in diameter and 1.0 inch in thickness were employed. The automated Porosimeter–Permeameter was used to measure the permeability and porosity.

Nuclear magnetic resonance

The impact of hydration on the pore size distribution and porosity variations for the cement specimens made from polypropylene was assessed using NMR. On cylindrical specimens with a 1.5 inches diameter and 4.0 inches length, the relaxation time (T_2) was measured using NMR with a weak magnetic field to produce easily detectable nuclear spin precession. Using a Geospec rock analyzer from Oxford Instruments (low magnetic field NMR), the T_2 relaxation time was measured (2 MHz).

Elasticity test

To determine how the curing period affected the elastic properties of all the specimens made from polypropylene, the Young's modulus and Poisson's ratio were determined. Utilizing the scratch test machine's sonic mode, cylindrical specimens with a length of 4.0 inches and a diameter of 1.5 inches were utilized to assess the cement's elastic capabilities. Following that, the ultrasonic velocities were measured in order to get the Young's modulus and Poisson's ratio (i.e., compressional and shear waves) (Ahmed et al. 2021a).

Density variation

Two portions of cylindrical samples with a 1.5 inches diameter and a 4.0 inches length were separated (bottom and top). Each component's weight, area, and length were all measured in order to estimate its density. The ratio of the density difference between the top and bottom of the sample to the density at the bottom was then used to calculate the density variation throughout the cement samples.

Results and discussion

The influence on the failure parameters

The compressive strengths of cement samples made from polypropylene fibers that were tested at various curing durations are summarized in Fig. 4. The compressive strength of the polypropylene and neat specimens rose over the first 48 h of curing but did not vary much after that point. At all curing durations, the samples with polypropylene fibers have higher compressive strengths compared to the base specimens.

The compressive strength of the base and polypropylene-based samples, as shown in Fig. 4a, is 44.5 MPa and 52.6 MPa, respectively, after 6 h of hydration. After a brief rise in strength, the basic cement's compressive strength gradually stabilized at about 51.5 MPa after 48 h. After 48 h of curing, the compressive strength of the polypropylene specimens likewise rose and stabilized, reaching 60.5 MPa. After 2 days of curing, the compressive strength of neither cement sample increased noticeably.

In order to establish the optimum mathematical connection that describes these changes, the variations in compressive strength of polypropylene and base specimens over time were examined. This study found that the logarithmic relationships of Eqs. (1) and (2), with (R^2) of 0.96 and 0.97, respectively, best represent variations in compressive strength for neat and polypropylene specimens as revealed in Fig. 4a.

$$UCS_{\text{base}} = 2.95\ln(T) + 39.9 \quad (1)$$

$$UCS_{\text{PPF}} = 3.41\ln(T) + 42.0 \quad (2)$$

Applying Eqs. (1) and (2) allowed us to track changes in both study systems' compressive strength over the period of 28 days, as depicted in Fig. 4b. According to this graph, the first week of curing is when both cement systems experienced the greatest changes in compressive strength. The compressive strength of polypropylene and base specimens changed very little after the first week, and after 21 days of curing, it had almost stabilized.

It is evident from the tensile strength data shown in Fig. 5 that the results for both systems' compressive and tensile strengths are equivalent. The tensile strength of polypropylene and base specimens grew as the early curing time increased, and the polypropylene-based cement's tensile strength was higher than the base cement's at all curing periods.

After 6 and 12 h, the polypropylene specimen's tensile strengths were 4.65 and 5.30 MPa, respectively, which were greater than the corresponding values for the base cement samples' tensile strengths of 4.06 and 4.36 MPa. The tensile strength of the polypropylene and base specimens then gradually increased and nearly stabilized after 48 h at 4.89 MPa for the neat cement and 6.06 MPa for the polypropylene specimen, respectively. After 72 h of curing, the tensile strengths of the neat and polypropylene specimens are 4.96 MPa and 6.25 MPa, respectively.

According to the results of the regression investigation, the variation in tensile strength of the neat and polypropylene specimens could be accurately represented with R^2 values of 0.99 and 0.97, respectively, with the help of logarithmic relationships of Eqs. (3) and (4), as illustrated in Fig. 5a.

$$TS_{\text{base}} = 0.37\ln(T) + 3.43 \quad (3)$$

$$TS_{\text{PPF}} = 0.63\ln(T) + 3.64 \quad (4)$$

The plots in Fig. 5b show how Eqs. (3) and (4) were applied to study the variations in tensile strength for all the specimens during the first 4 weeks of curing. The majority of the growth of the tensile strength of the polypropylene and base specimens occurred during the first 7 days of hydration, after which there was only a minor growth in the tensile strength, which tends to be constant after 3 weeks for the base specimens and 24 days for the polypropylene specimens.

The influence on the petrophysical properties

The results of measuring the permeability of all cement specimens are displayed in Fig. 6. These results showed that

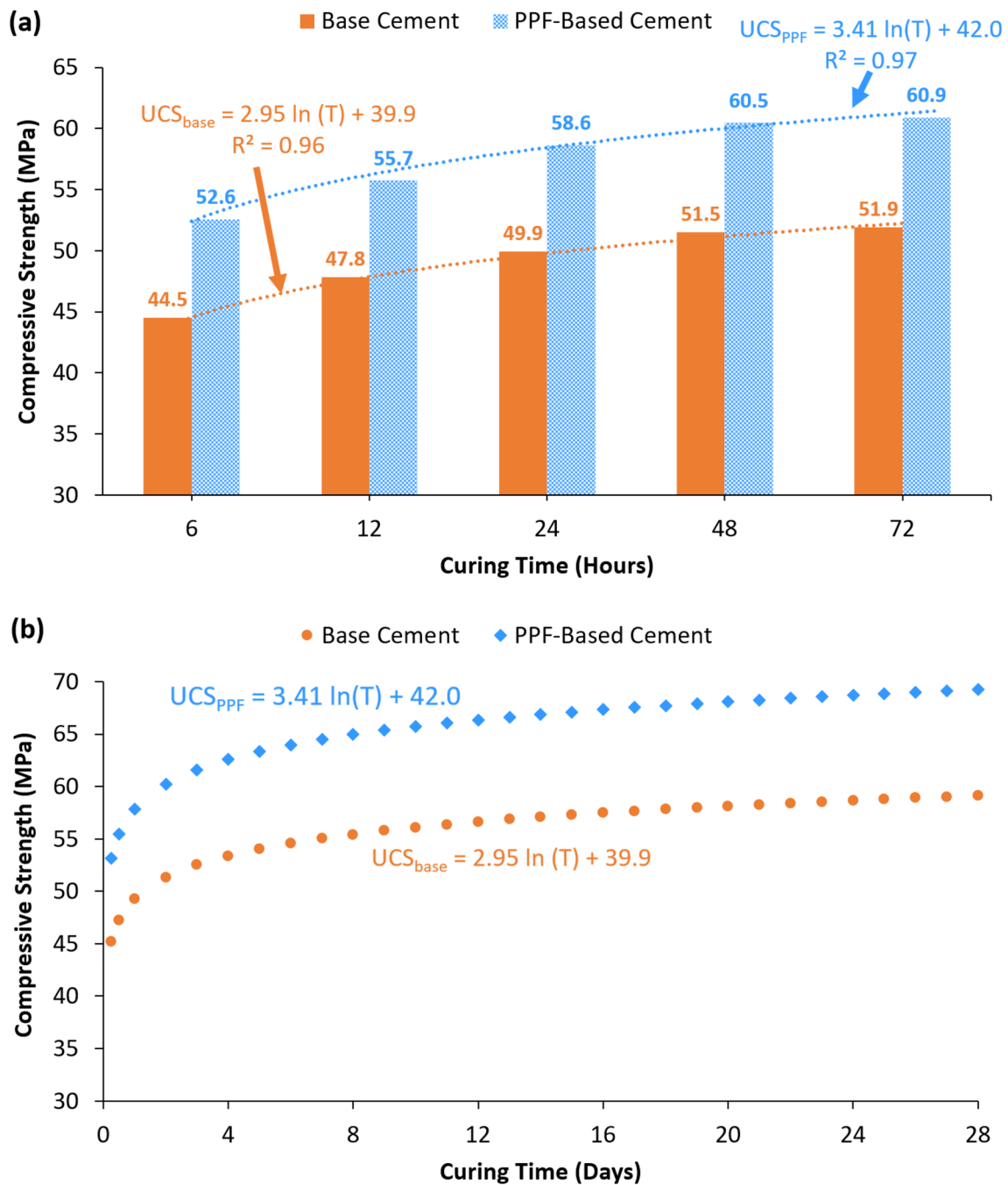


Fig. 4 Compressive strength for the polypropylene and base specimens at various curing times. **a** The findings of the compressive strengths during early curing times. **b** The anticipated variations in compressive strength over 4 weeks

with increasing curing time, the permeability of neat and polypropylene cement specimens reduced. The permeability of the polypropylene specimens was, however, lower than that of the base cement.

The results in Fig. 6 demonstrate that the permeability of the neat specimen was 0.059 mD after six hours of curing. This permeability rapidly reduced with curing time, and the neat specimen was 0.026 mD after 72 of hydration. The

polypropylene-based cement showed a similar tendency; it had a permeability of 0.050 mD after 6 h of curing and was rapidly losing permeability throughout the first 24 h of curing before tending to stabilize at 0.022 mD after curing.

In order to find the optimum mathematical connection to reflect these changes, it was also explored how the permeability of the base and polypropylene specimens changed with the hydration process. The results demonstrated that

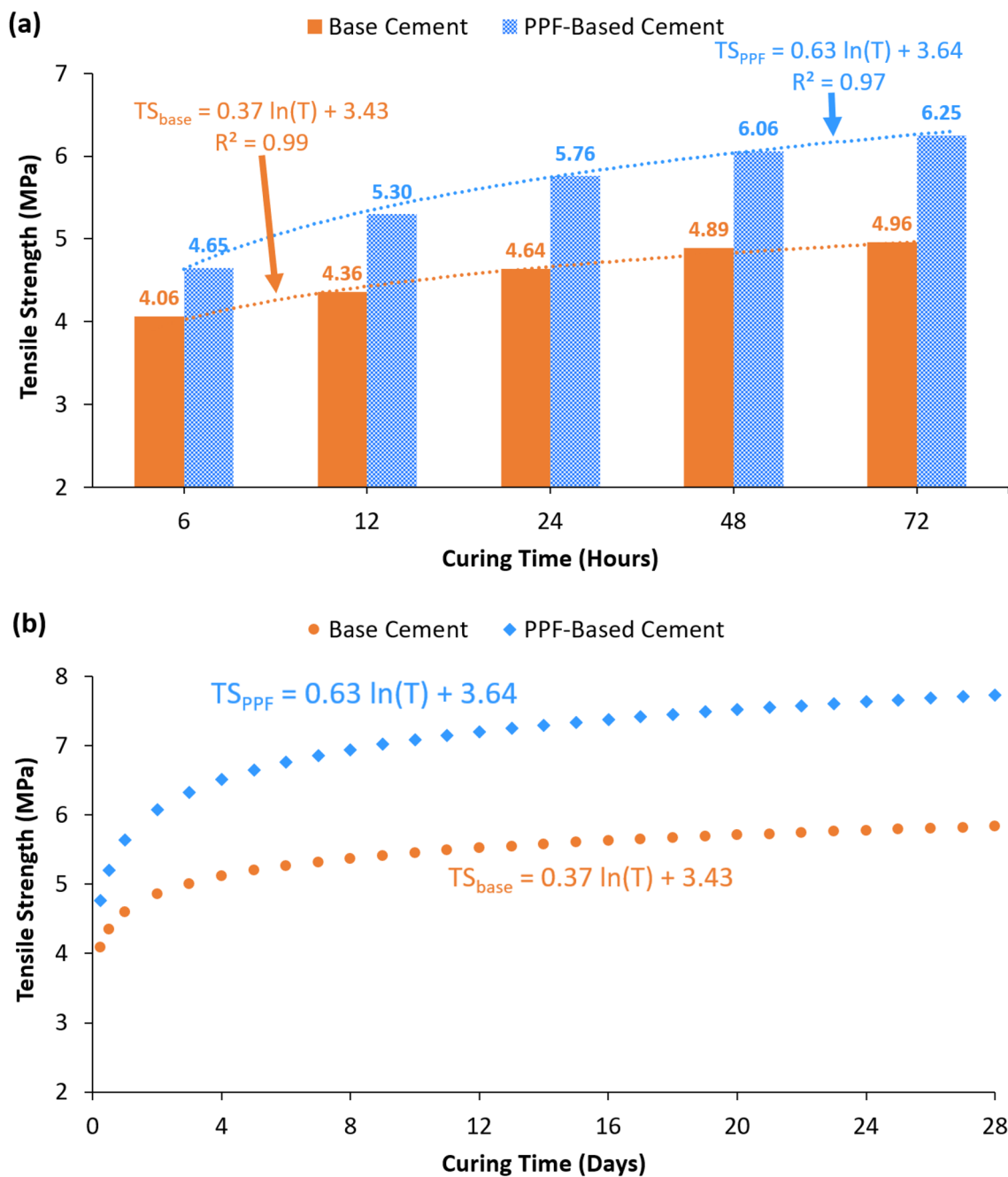


Fig. 5 Tensile strength for the polypropylene and base specimens at various stages of curing. **a** The findings of the tensile strength during the early curing times. **b** The anticipated variations in tensile strength over 4 weeks

the power relationships of Eqs. (5) and (6), with R^2 values of 0.992 and 0.997, respectively, best represent the increases in permeability for the base and polypropylene specimens, as demonstrated in Fig. 6a.

$$K_{base} = 0.107T^{-0.327} \tag{5}$$

$$K_{PPF} = 0.088T^{-0.325} \tag{6}$$

Using Eqs. (5) and (6), the variations in the permeability of the base and polypropylene specimens for the first 4 weeks of curing were then determined, as revealed in Fig. 6b. This graph demonstrates how both cement systems' permeability significantly decreased within the first week. Although at a slower rate than the first week of cure, the

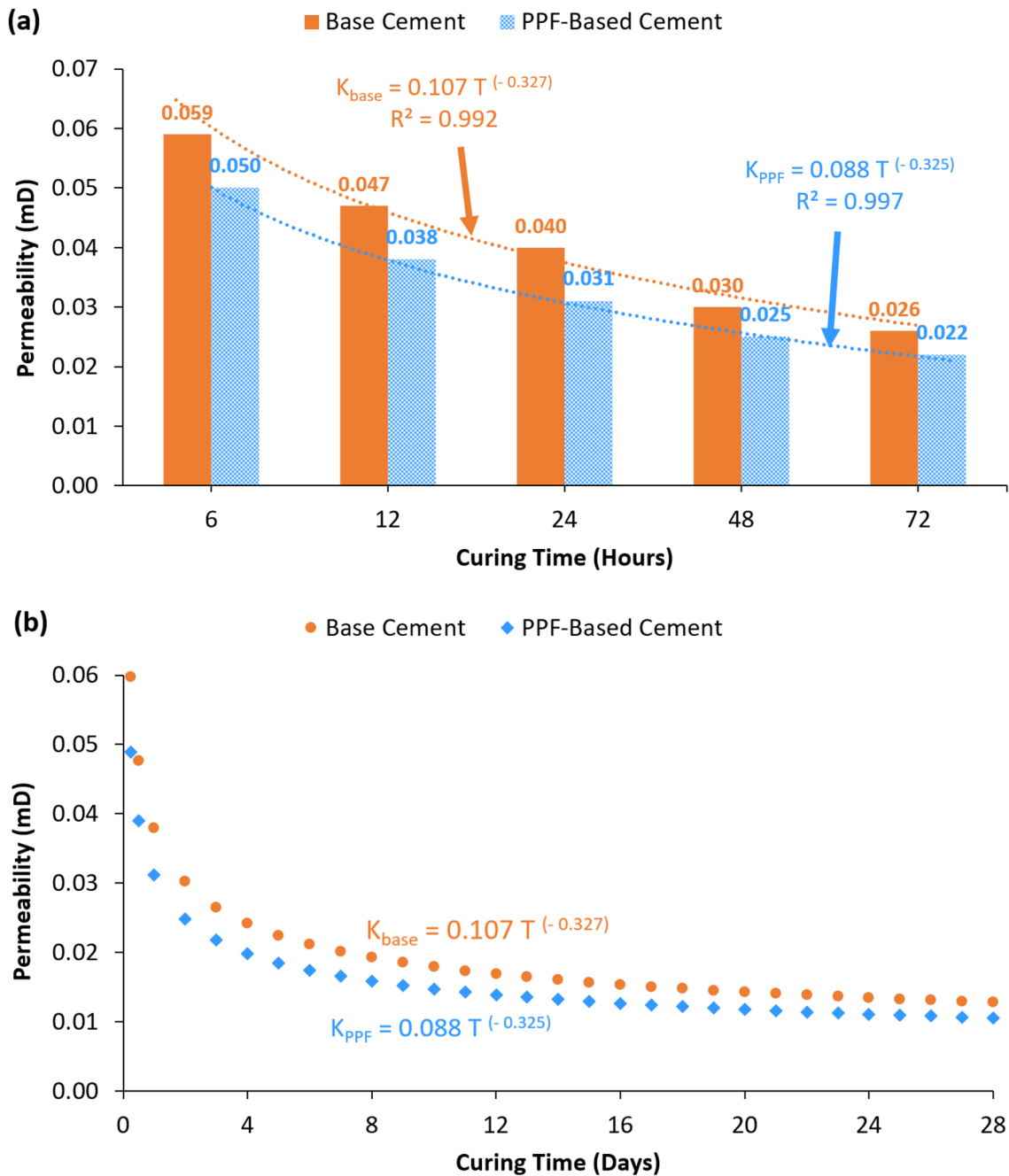


Fig. 6 Permeability for polypropylene and base specimens at various stages of curing. **a** The findings of the permeability during the early curing times. **b** The anticipated variations in permeability over 4 weeks

permeability continued to decrease until the conclusion of week three. The permeability of both samples stabilized after 24 days of cure.

Following 6, 12, 24, 48, and 72 h of curing time, Fig. 7 illustrates the porosity of the cement specimens for the two cement systems with and without polypropylene fibers. It was evident that as the curing period grew, so did the porosities of the base and polypropylene systems. For all of the

applied curing durations, the polypropylene cement's porosity was less than the base cement's porosity.

For the base specimens, the porosity was 15.3% after 6 h and significantly increased to stabilize at 21.2% after 48 h of hydration. After 6 h of hydration, the polypropylene-based samples' porosity was 13.9%; after 2 days of curing, it stabilized at 19.2%. The porosity for both systems did not significantly change, though, and stabilized

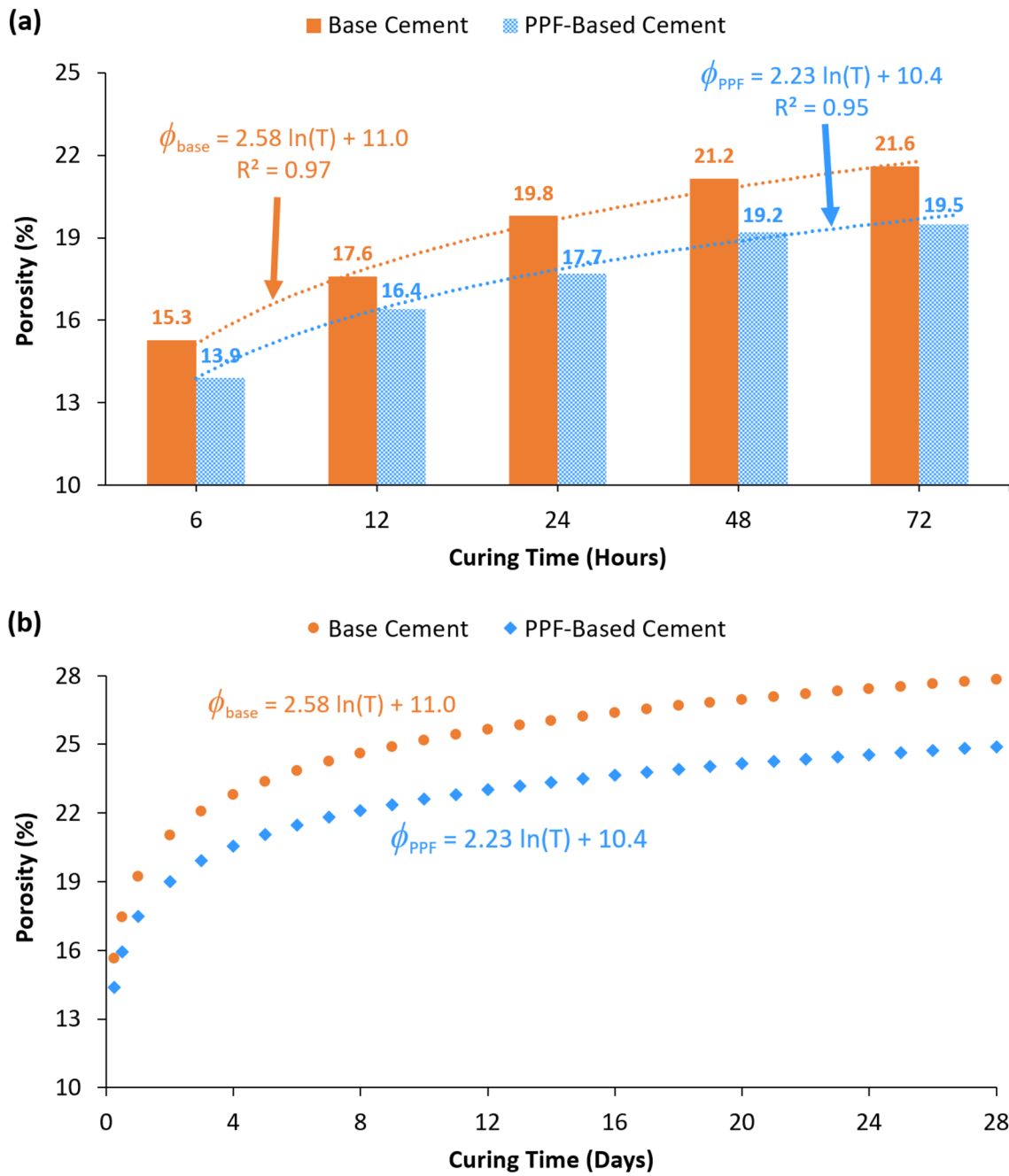


Fig. 7 Porosity for the polypropylene and base specimens at various stages of curing. **a** The findings of the porosity measurements during the early curing times. **b** The anticipated variations in porosity over 4 weeks

at 21.6% and 19.5% for the base and polypropylene specimens, respectively, after three days of hydration.

Regression analysis revealed that the logarithmic relationships of Eqs. (7) and (8), with R^2 values of 0.97 and 0.95, respectively, could accurately characterize the variation in porosity of the base and polypropylene specimens, as presented in Fig. 7a.

$$\phi_{\text{base}} = 2.58 \ln(T) + 11.0 \tag{7}$$

$$\phi_{\text{PPF}} = 2.23 \ln(T) + 10.4 \tag{8}$$

The variations in porosity for the base and polypropylene specimens over the first 4 weeks of curing were

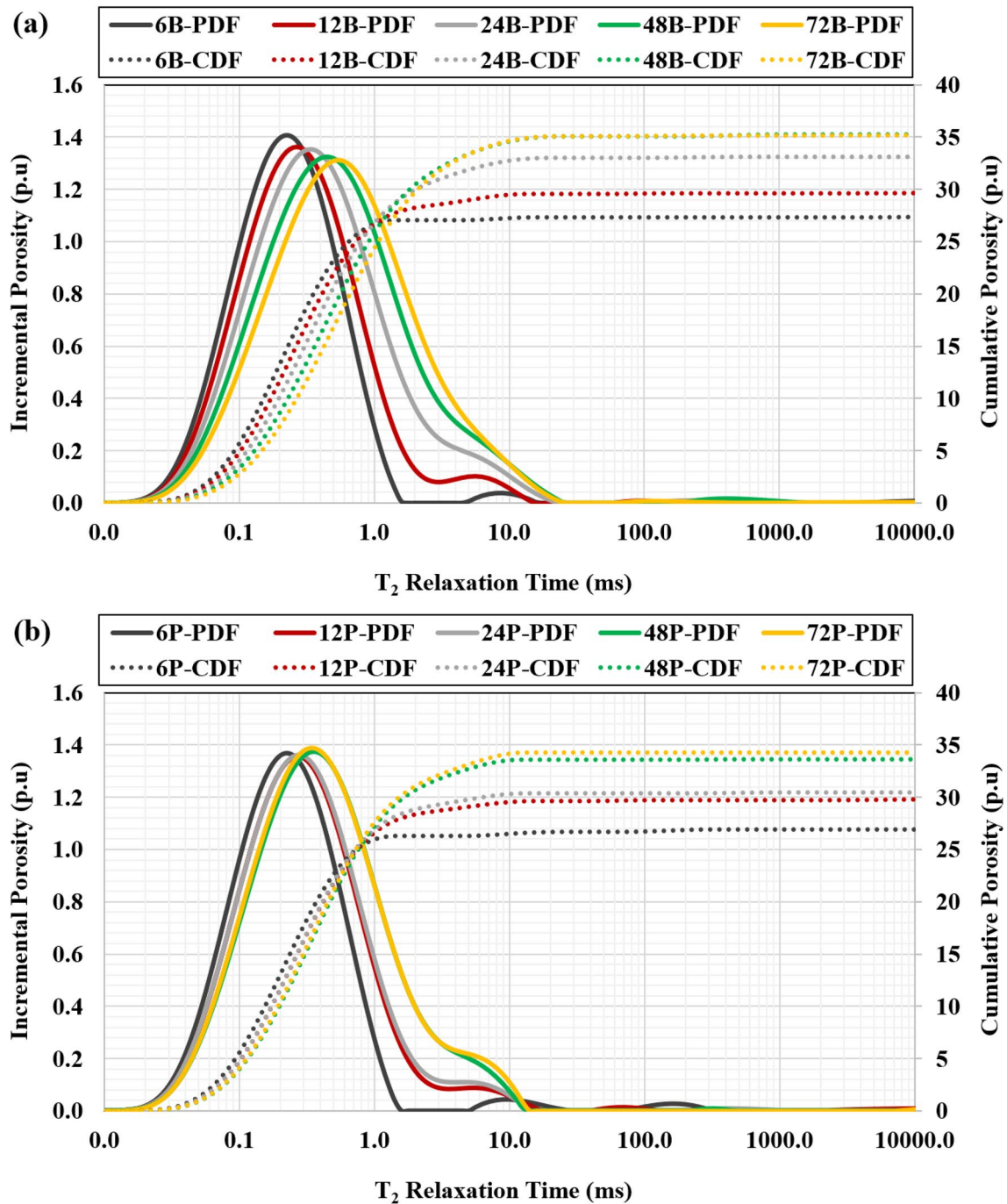


Fig. 8 NMR T_2 relaxation for **a** neat cement specimens and **b** polypropylene specimens, after 6, 12, 24, 48, and 72 h of hydration

then plotted using Eqs. (7) and (8), as seen in the plots of Fig. 7b. As shown in this figure, both cement systems' porosity significantly increased throughout the first seven days of hydration as the curing period increased. After 24 days of hydration, this rate of growth moderated and the porosity tended to settle.

NMR characterization

NMR was used to carefully examine how the two cement systems' pore size distribution was affected by the curing time. Additionally, Fig. 8a for the base cement samples and Fig. 8b for the polypropylene cement samples show

the PDF and CDF throughout the entire length of the cement specimen (4 inches). The findings demonstrated that for both systems, the porosity of the samples rose at a decreasing rate as the curing period increased until the end of the initial 48 h of curing. For instance, the porosities in the base cement samples (Fig. 8a) were 27.4%, 29.7%, 33.1%, 35.2%, and 35.3%, respectively, at 6, 12, 24, 48, and 72 h of curing. The same pattern was seen in cement

samples made of polypropylene (Fig. 8b), where the porosities were 26.9%, 29.8%, 30.5%, 33.6%, and 34.3% after 6, 12, 24, 48, and 72 h of curing. Although the values of NMR porosities are unlike the porosities attained from gas Porosimeter, it can be seen that they follow a similar trend in Fig. 7. Here, porosity increases with an increase in curing time, and the porosities of polypropylene cement

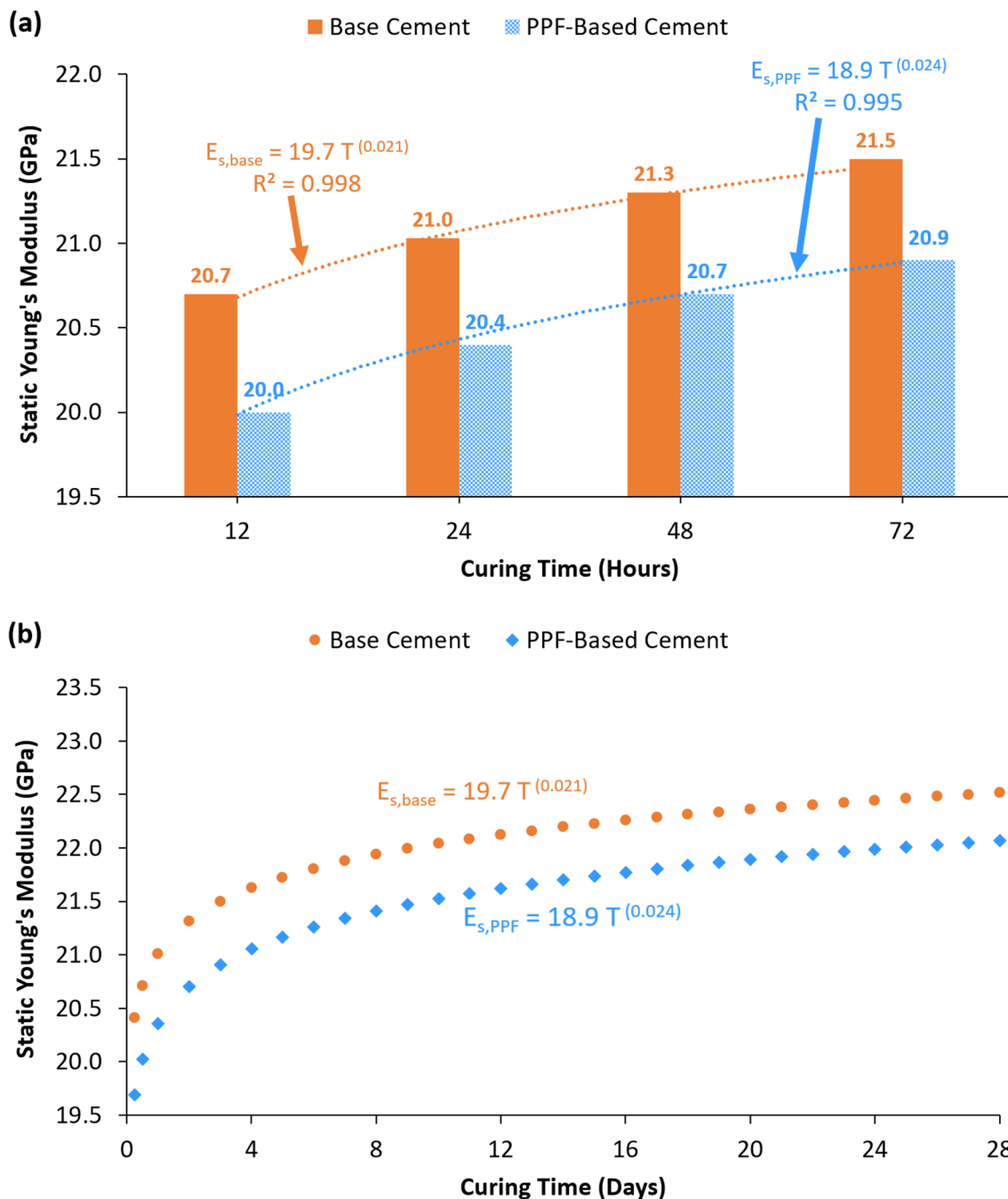


Fig. 9 Young's modulus for polypropylene and base specimens at various stages of curing. **a** The findings of the Young's modulus during the early curing times. **b** The anticipated variations in Young's modulus over 4 weeks

are lower than the porosity of base cement, despite the fact that the measurement methods are different.

The influence on elastic properties

The two most significant elastic properties of solid materials are believed to be Young's modulus and Poisson's ratio. When the Young's modulus is low, the cement is more stable under shear loads, and when the Poisson's ratio is high, the cement is less expandable (Fajer et al. 2008). Figure 9 shows how the hydration time affects the Young's modulus of neat and polypropylene specimens. The samples of base and polypropylene specimens had Young's moduli of 20.7 MPa and 20.0 MPa, respectively, after 12 h of curing. After 72 h of hydration, the Young's modulus was then gradually raised to stabilize at 21.5 MPa for the neat specimen and 20.9 MPa for the polypropylene specimen. The drop in Young's modulus for the samples made with polypropylene fiber supported these findings, which showed that adding polypropylene fiber made the cement matrix more stable under shear stresses.

Mathematical analysis was done to determine the appropriate connection to describe the variations in Young's modulus of the neat and polypropylene specimens with respect to curing time. The results demonstrated that the power relationships of Eqs. (9) and (10) with R^2 values of 0.998 and 0.995, respectively, for the base and polypropylene specimens, best represent the variations in Young's modulus, as illustrated in Fig. 9a.

$$E_{s,\text{base}} = 19.77T^{0.021} \quad (9)$$

$$E_{s,\text{PPF}} = 18.97T^{0.024} \quad (10)$$

Equations (9) and (10), respectively, were then applied to determine the variations in Young's modulus of the neat and polypropylene specimens for the first 4 weeks of curing, as depicted in Fig. 9b. This graph demonstrates that both cement systems' Young's modulus increased significantly during the first week. Young's modulus continued to rise throughout the final 24 days, though at a slower rate than during the first week of curing. Young's modulus of the neat and polypropylene specimens stabilized after 24 days of curing.

After 12 h of curing, the Poisson's ratio, as presented in Fig. 10a, was 0.272 for the neat specimen and 0.280 for the polypropylene specimen. After three days of hydration, the Poisson's ratio for the neat and polypropylene specimens, respectively, decreased steadily with curing time to reach 0.256 and 0.268. The Poisson's ratio results in Fig. 10a demonstrated that the polypropylene-based samples had greater Poisson's ratios than the neat specimens did at the

four curing times, indicating that these samples had strong elasticity and little lateral expandability.

Regression analysis was used to evaluate the Poisson's ratio variations with curing time for neat and polypropylene specimens in order to determine the most appropriate relationship to depict these variations. The results demonstrated that the power relationships of Eqs. (11) and (12), with R^2 values of 0.99 and 0.98, respectively, best represent the variations in Poisson's ratio for the neat and polypropylene specimens, as revealed in Fig. 10a.

$$\nu_{\text{base}} = 0.297T^{-0.036} \quad (11)$$

$$\nu_{\text{PPF}} = 0.297T^{-0.025} \quad (12)$$

Using Eqs. (11) and (12), the variations in the Poisson's ratio for the neat and polypropylene specimens over the first four weeks of curing were then determined, as presented in Fig. 10b. This graph demonstrates the significant decline in Poisson's ratio that base and polypropylene specimens underwent between 12 h and 7 days of curing. Although at a slower rate than the first week of hydration, Poisson's ratio continued to fall until the middle of the 28 days. Poisson's ratios for both samples stabilized after 24 days of curing.

The influence on the density variation

Due to the solid particles at the bottom of the cement column settling, the density variation over the height of the cement paste is frequently not the same. Therefore, it is crucial to examine the density variation (DV) as a function of the hydration period for the base and polypropylene specimens as well as the DV between the top and bottom of the specimens.

The density variation for the neat and polypropylene specimens after 12 h of curing is 4.9% and 4.1%, respectively, as shown in Fig. 11a. For the following two and a half days, the density variation was dramatically reduced to reach 3.2% and 2.6% for the neat and polypropylene specimens, respectively.

According to the regression analysis, the power relationships of Eqs. (13) and (14) with R^2 values of 0.99 and 0.97, respectively, could accurately represent the variation in the density variation of the base (neat) and polypropylene specimens, as revealed in Fig. 11a.

$$DV_{\text{base}} = 8.76T^{-0.24} \quad (13)$$

$$DV_{\text{PPF}} = 7.42T^{-0.25} \quad (14)$$

The variations in the density variation for the neat and polypropylene specimens throughout the first four weeks

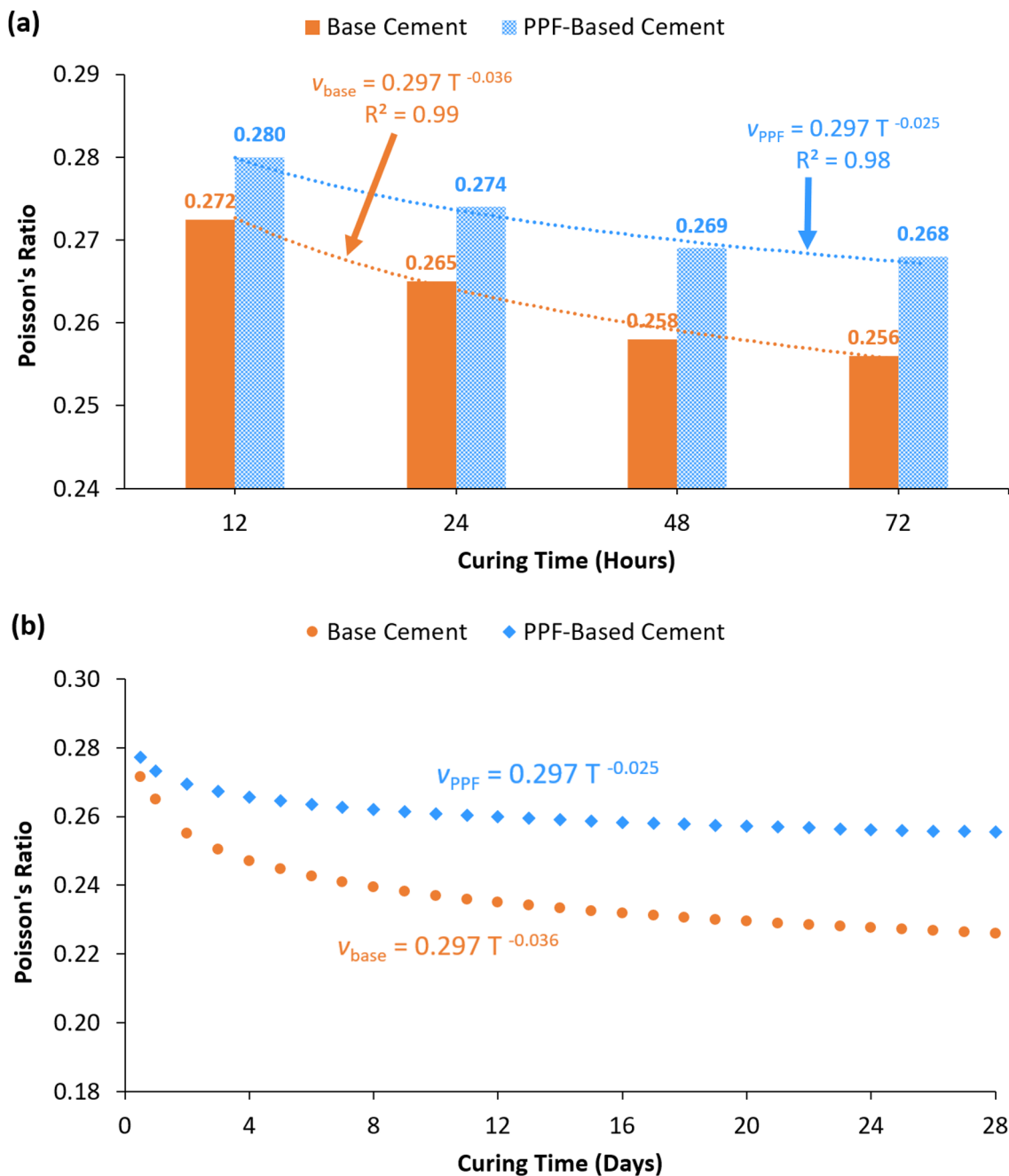


Fig. 10 Poisson's ratio for the polypropylene and base specimens at various stages of curing. **a** The findings of the Poisson's ratio during the early curing times. **b** The anticipated variations in Poisson's ratio over 4 weeks

of curing were then plotted using Eqs. (13) and (14) as illustrated by the plots of Fig. 11b. As seen in this figure, the density variation for the neat and polypropylene specimens significantly decreased over the first seven days of hydration as the curing period increased. After 24 days of hydration, this rate of decline slowed down and the density variation tended to settle.

Conclusions

In this study, a novel work has been conducted by investigating the influence of polypropylene fiber on the change of the early properties of class G oil well cement. Cement samples containing polypropylene fiber and neat cement samples (without polypropylene fiber) were cured at five

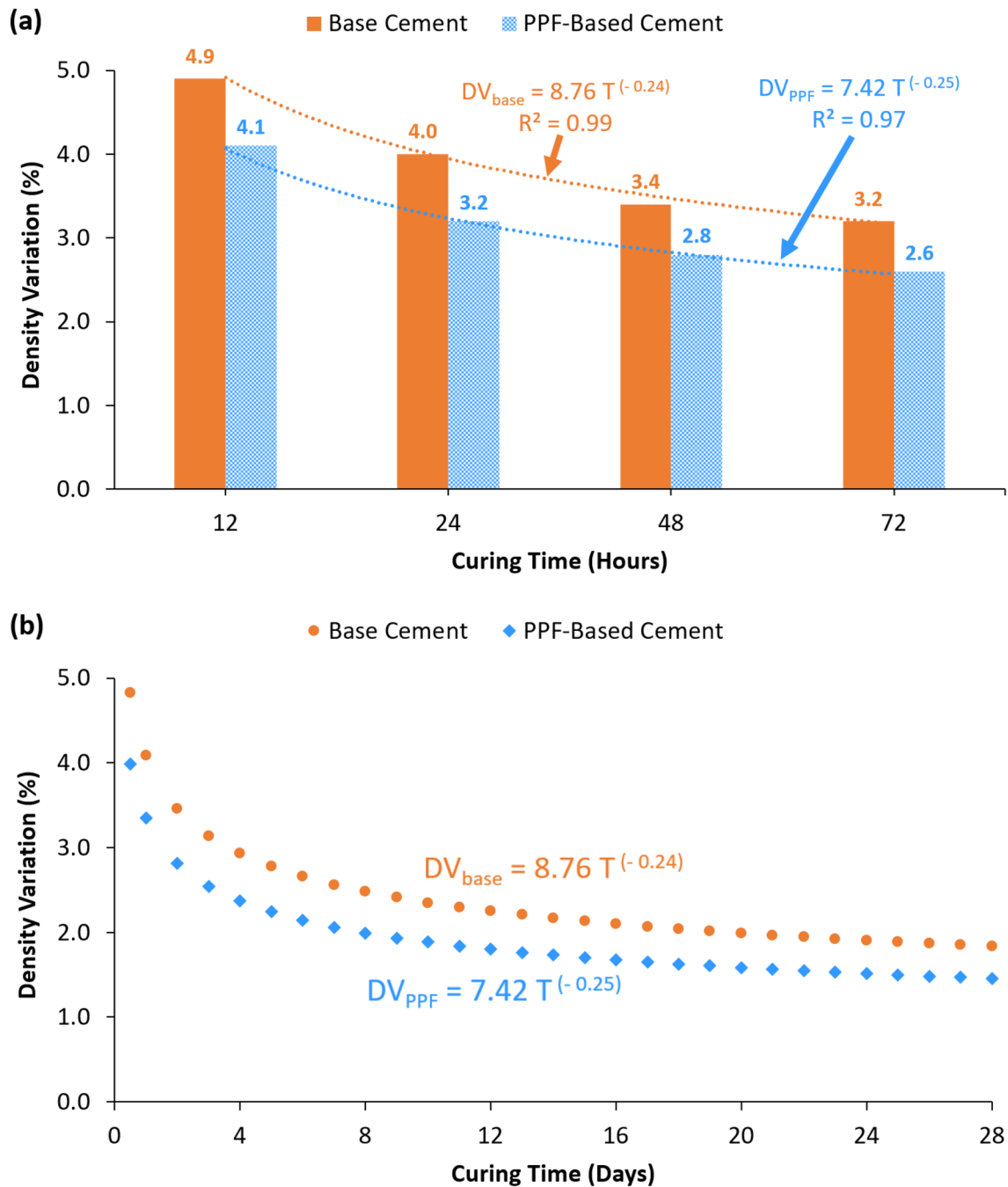


Fig. 11 Density variation for the polypropylene and base specimens at various stages of curing. **a** The findings of the density variation during the early curing times. **b** The anticipated density variation over 4 weeks

separate curing processes lasting 6, 12, 24, 48, and 72 h each, after which the changes in their characteristics were assessed. The results lead to the following conclusions:

- In comparison with the strengths of a neat specimens, the addition of polypropylene fiber enhanced the compressive strength by 17.3% and the tensile strength by 26%. The strength of the neat and polypropylene specimens also increased as the curing period increased.
- In comparison with neat cement, the addition of polypropylene fiber reduced the cement matrix's permeability and porosity by 15% and 9.7%, respectively.

- The cement's elasticity was also improved by the addition of polypropylene fiber, as shown by a 2.8% reduction in Young's modulus and a 4.7% increase in Poisson's ratio.
- In addition to porosity, logarithmic relationships were constructed to indicate variations in compressive and tensile strength. While the Poisson's ratio, Young's modulus, and density fluctuation variations in the other permeability parameters were accurately modeled by power-law equations.

Acknowledgements The authors would like to thank King Fahd University of Petroleum and Minerals (KFUPM) for employing its resources in conducting this work.

Funding This research received no external funding.

Declarations

Conflict of interest The authors declare that there is no conflict of interest regarding the publication of this paper.

Open Access This article is licensed under a Creative Commons Attribution 4.0 International License, which permits use, sharing, adaptation, distribution and reproduction in any medium or format, as long as you give appropriate credit to the original author(s) and the source, provide a link to the Creative Commons licence, and indicate if changes were made. The images or other third party material in this article are included in the article's Creative Commons licence, unless indicated otherwise in a credit line to the material. If material is not included in the article's Creative Commons licence and your intended use is not permitted by statutory regulation or exceeds the permitted use, you will need to obtain permission directly from the copyright holder. To view a copy of this licence, visit <http://creativecommons.org/licenses/by/4.0/>.

References

- Agofack N, Ghabezloo S, Sulem J et al (2019) Experimental investigation of the early-age mechanical behaviour of oil-well cement paste. *Cem Concr Res* 117:91–102. <https://doi.org/10.1016/j.cemconres.2019.01.001>
- Ahmed A, Elkhatatny S, Gajbhiye R, et al (2018) Effect of polypropylene fibers on oil-well cement properties at HPHT condition. In: Soc Pet Eng—SPE Kingdom of Saudi Arabia annual technical symposium and exhibition 2018, SATS 2018. <https://doi.org/10.2118/192187-ms>
- Ahmed A, Bageri B, Al Jaber J, et al (2021a) Improvement of well cementing properties using perlite particles. In: 55th US rock mechanics/geomechanics symposium, vol 3, pp 652–657
- Ahmed A, Mahmoud AA, Elkhatatny S, et al (2021b) Application of tire waste material to enhance the properties of Saudi class G oil well cement. In: SPE Middle east oil & gas show and conference MEOS, Proceedings, <https://doi.org/10.2118/204788-MS>
- Ahmed A, Mahmoud AA, Elkhatatny S, Al-Majed A (2021c) Evaluation of Granite Waste and Silica Flour in Oil Well Cementing. In: 55th U.S. rock mechanics/geomechanics symposium, vol 3, pp 646–651
- Al Maskary S, Halim AA, Al Menhali S (2014) Curing losses while drilling & cementing. In: Soc Pet Eng—30th Abu Dhabi international petroleum exhibition and conference ADIPEC 2014 Challenges Oppor Next 30 Years, vol 4, pp 2492–2497. <https://doi.org/10.2118/171910-ms>
- API (1997) Recommended practice for testing well cements API recommended practice 10B-2. 171
- ASTM (2001) Standard test method for splitting tensile strength of intact rock core specimens 1
- ASTM (2020) Standard test method for compressive strength of hydraulic cement mortars
- Bageri B, Ahmed A, Al Jaber J et al (2021) Effect of perlite particles on the properties of oil-well class G cement. *J Pet Sci Eng* 199:108344. <https://doi.org/10.1016/j.petrol.2021.108344>
- Bentur A, Mindess S (2020) Introduction. Fibre reinforced cement composites. IntechOpen, pp 21–30
- Elkhatatny S, Gajbhiye R, Ahmed A, Mahmoud AA (2020) Enhancing the cement quality using polypropylene fiber. *J Pet Explor Prod Technol*. <https://doi.org/10.1007/s13202-019-00804-4>
- Elmoneim HA, Zaki S, Al-Arda H (2000) Cementing the deepest 20 inch Casing in Abu Dhabi using a combination of noval light weight slurry and fiber. In: Soc Pet Eng—Abu Dhabi international petroleum exhibition and conference 2000, ADIPEC 2000. <https://doi.org/10.2118/87283-ms>
- Fajer E, Hokt R, Horsrud P et al (2008) Petroleum related rock mechanics. Elsevier
- Ilyas M, Sadiq N, Mughal MA, et al (2012) Improvement of cementing in deep wells. In: Soc Pet Eng—SPE/PAPG annual technical conference 2012, PATC 2012, pp 155–172. <https://doi.org/10.2118/163128-ms>
- Iremonger SS, Bolt M, Lawrence SC (2015) Enhanced thermal well integrity through the use of a new cement tensile strength-enhancing fiber. In: Soc Pet Eng—SPE Canada heavy oil technical conference 2015, CHOC 2015, pp 246–257. <https://doi.org/10.2118/174483-ms>
- Jamshidi M, Karimi M (2019) Characterization of polymeric fibers as reinforcements of cement-based composites. *J Appl Polym Sci*. <https://doi.org/10.1002/app.30302>
- Jo BW, Kim CH, Tae GH, Park JB (2007) Characteristics of cement mortar with nano-SiO₂ particles. *Constr Build Mater* 21:1351–1355. <https://doi.org/10.1016/j.conbuildmat.2005.12.020>
- Krakowiak KJ, Thomas JJ, Musso S et al (2015) Nano-chemo-mechanical signature of conventional oil-well cement systems: effects of elevated temperature and curing time. *Cem Concr Res* 67:103–121. <https://doi.org/10.1016/j.cemconres.2014.08.008>
- Liu X, Wang R, Wu Z, Liu W (2012) The effect of triangle-shape carbon fiber on the flexural properties of the carbon fiber reinforced plastics. *Mater Lett* 73:21–23. <https://doi.org/10.1016/j.matlet.2012.01.003>
- Lyomov SK, Backe KR, Skalle P, et al (1997) Shrinkage of oil well cement slurries. Annu Tech Meet 1997, ATM 1997. <https://doi.org/10.2118/98-09-06>
- Mahmoud AA, Elkhatatny S (2019) The effect of silica content on the changes in the mechanical properties of class G cement at high temperature from slurry to set. In: 53rd U.S. rock mechanics/geomechanics symposium, pp 1–5
- Mahmoud AA, Elkhatatny S (2020) Improving class G cement carbonation resistance for applications of geologic carbon sequestration using synthetic polypropylene fiber. *J Nat Gas Sci Eng* 76:103184. <https://doi.org/10.1016/j.jngse.2020.103184>
- Mahmoud AA, Elkhatatny S, Ahmed A, et al (2018) SPE-193059-MS Nanoclay content influence on cement strength for oil wells subjected to cyclic steam injection and high-temperature conditions
- Messier E, Stiles D, Morgan R (2002) Controlling cement tops through use of fiber-based slurries reduces drilling costs. In: Canadian international petroleum conference 2002, CIPC 2002, vol 42. <https://doi.org/10.2118/2002-085>
- Nelson E, Guillot D (2006) Well cementing. Schlumberger

- Parcevaux PA, Sault PH (1984) Cement shrinkage and elasticity: A new approach for a good zonal isolation. Proceedings of the SPE annual technical conference and exhibition. <https://doi.org/10.2523/13176-ms>
- Park SJ, Seo MK, Shim HB (2003) Effect of fiber shapes on physical characteristics of non-circular carbon fibers-reinforced composites. *Mater Sci Eng A* 352:34–39. [https://doi.org/10.1016/S0921-5093\(02\)00463-X](https://doi.org/10.1016/S0921-5093(02)00463-X)
- Parrott LJ, Geiker M, Gutteridge WA, Killoh D (1990) Monitoring Portland cement hydration: comparison of methods. *Cem Concr Res* 20:919–926. [https://doi.org/10.1016/0008-8846\(90\)90054-2](https://doi.org/10.1016/0008-8846(90)90054-2)
- Puppala AJ, Musenda C (2000) Effects of fiber reinforcement on strength and volume change in expansive soils. *Transp Res Rec C*:134–140. <https://doi.org/10.3141/1736-17>
- Reinås L, Hodne H, Turkel MA (2011) Hindered strength development in oil well cement due to low curing temperature. In: *Soc Pet Eng—Arctic and extreme environments conference and exhibition 2011*, vol 1, pp 380–406. <https://doi.org/10.2118/149687-ms>
- Sant G, Dehadrai M, Bentz D et al (2009) Detecting the transition in cement pastes comparing experimental and numerical techniques. *Concr Int* 31:53–58
- Shi G, Liu W, Gao Y (1995) Modifying set cement performance for improving cementing job quality. *Proc Int Meet Pet Eng* 1:335–342. <https://doi.org/10.2523/29924-ms>
- Sobolev K, Gutiérrez MF (2005) How nanotechnology can change the concrete world. *Am Ceram Soc Bull* 84:14–18. <https://doi.org/10.1002/9780470588260.ch17>
- Tang C, Shi B, Gao W et al (2007) Strength and mechanical behavior of short polypropylene fiber reinforced and cement stabilized clayey soil. *Geotext Geomembr* 25:194–202. <https://doi.org/10.1016/j.geotexmem.2006.11.002>
- Thiercelin MJ, Dargaud B, Baret JF, Rodriguez WJ (1997) Cement design based on cement mechanical response
- Thomas JJ, Jennings HM, Chen JJ (2009) Influence of nucleation seeding on the hydration mechanisms of Tricalcium silicate and cement. *J Phys Chem C* 113:4327–4334. <https://doi.org/10.1021/jp809811w>
- Vandewalle L (2007) Postcracking behaviour of hybrid steel fiber reinforced concrete. In: *Proceedings of the 6th international conference fracture mechanics of concrete and concrete structures*, vol 3, pp 1367–1375
- Vasudev D (2007) Performance studies on rigid pavement sections built on stabilized sulfate soils
- Viswanadham BVS, Phanikumar BR, Mukherjee RV (2009) Swelling behaviour of a geofiber-reinforced expansive soil. *Geotext Geomembr* 27:73–76. <https://doi.org/10.1016/j.geotexmem.2008.06.002>
- Yao W, Li J, Wu K (2003) Mechanical properties of hybrid fiber-reinforced concrete at low fiber volume fraction. *Cem Concr Res* 33:27–30. [https://doi.org/10.1016/S0008-8846\(02\)00913-4](https://doi.org/10.1016/S0008-8846(02)00913-4)
- Yetimoglu T, Inanir M, Inanir OE (2005) A study on bearing capacity of randomly distributed fiber-reinforced sand fills overlying soft clay. *Geotext Geomembr* 23:174–183. <https://doi.org/10.1016/j.geotexmem.2004.09.004>

Publisher's Note Springer Nature remains neutral with regard to jurisdictional claims in published maps and institutional affiliations.